

HIGH-TEMPERATURE MODAL SURVEY OF A HOT-STRUCTURE CONTROL SURFACE

Natalie D. Spivey

NASA Dryden Flight Research Center, Edwards, California, USA

Keywords: *Modal survey, ground vibration test, high-temperature, aerothermoelastic, hot-structure control surface*

Abstract

Ground vibration tests are routinely conducted for supporting flutter analysis for subsonic and supersonic vehicles; however, for hypersonic vehicles, thermoelastic vibration testing techniques are neither well established nor routinely performed. New high-temperature material systems, fabrication technologies and high-temperature sensors expand the opportunities to develop advanced techniques for performing ground vibration tests at elevated temperatures.

When high-temperature materials, which increase in stiffness when heated, are incorporated into a hot-structure which contains metallic components that decrease in stiffness when heated, the interaction between those materials can affect the hypersonic flutter analysis. A high-temperature modal survey will expand the research database for hypersonics and improve the understanding of this dual-material interaction.

This paper discusses the vibration testing of the carbon-silicon carbide Ruddervator Subcomponent Test Article, which is a truncated version of a full-scale hot-structure control surface. Two series of room-temperature modal test configurations were performed in order to define the modal characteristics of the test article during the elevated-temperature modal survey: one with the test article suspended from a bungee cord (free-free) and the second with it mounted on the strongback (fixed boundary). Testing was performed in the NASA Dryden Flight Research Center Flight Loads Laboratory Large Nitrogen Test Chamber.

1 Introduction

The National Aeronautics and Space Administration [NASA] Dryden Flight Research Center [DFRC] (Edwards, California, USA) directed a program to test a carbon-silicon carbide [C/SiC] Ruddervator Subcomponent Test Article [RSTA] to support the research objectives of the Fundamental Aeronautics Program within the hypersonics materials and structures disciplines. The C/SiC RSTA high-temperature testing provides opportunities to evaluate the performance of a C/SiC hot-structure control surface under re-entry and hypersonic cruise test conditions and to evaluate the performance of advanced high-temperature instrumentation. The RSTA underwent numerous thermal, thermal-mechanical and thermal-vibration tests to develop an extensive database for future structural design and analysis methodology validation. This paper discusses the three modal surveys that were conducted in attempting to understand the thermoelastic interaction of a hot-structure control surface.

1.1 The Carbon-silicon Carbide Ruddervator Subcomponent Test Article

In the early 2000s The Boeing Company (Chicago, Illinois, USA) and the Defense Advanced Research Projects Agency [DARPA] were developing the X-37 Orbital Test Vehicle, which would be launched into orbit from an expendable launch vehicle and be capable of returning to earth and landing autonomously [1]. In addition to vehicle development, program objectives focused on raising the

readiness level of certain technologies required for the vehicle. Development and validation testing of hot-structure control surfaces was a key enabling technology, because the X-37 had four hot-structure control surfaces: two flaperons and two ruddervators (see figure 1).

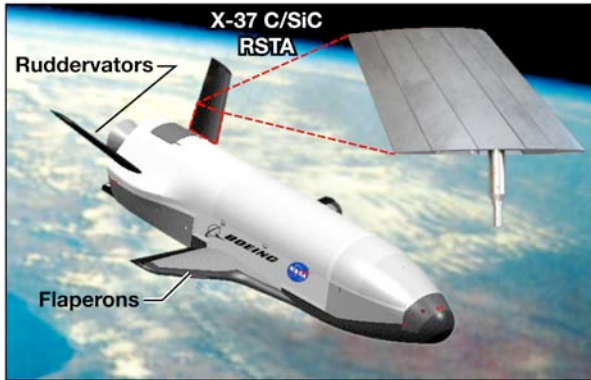


Fig. 1. The Hot-Structure Control Surfaces on the X-37 Orbital Test Vehicle.

These four surfaces were designed as load-bearing control surfaces capable of withstanding launch loads and the extreme re-entry thermal environment without using active cooling or thermal protection while retaining oxidation resistance and reusability. Two candidate materials (carbon-carbon and C/SiC) were selected for the control surfaces as a risk reduction during the technology development effort.

Under the X-37 technology development program a C/SiC RSTA, a truncated version of the full-scale X-37 hot-structure control surface, was designed and fabricated but not tested. The C/SiC RSTA was used in the recent research and test program at NASA DFRC. The 68-lb (30.8-kg) RSTA duplicated the outer mold line and encompassed the major features of the full-scale structure (the metallic spindle, the number and layout of the C/SiC components, spar boxes and C/SiC fasteners). The C/SiC RSTA is shown in figure 2.

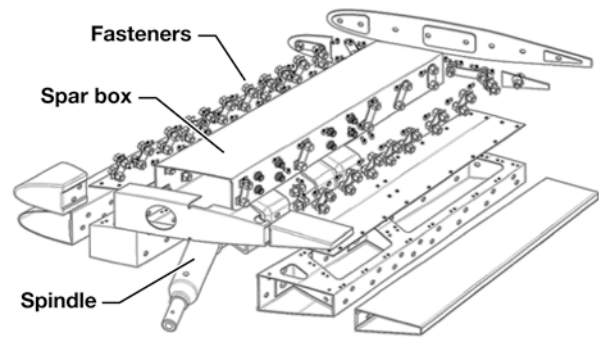


Fig. 2. The X-37 Carbon-Silicon Carbide Ruddervator Subcomponent Test Article Subcomponent Assembly.

1.2 Modal Survey Testing at Elevated Temperatures

Hypersonic vehicles experience extreme aerodynamic heating, extremely high surface temperatures and large temperature gradients. All of these can affect the structural integrity and the aeroelastic and aeroservoelastic stability of the vehicle. The reliability of analytical methods to predict these stability changes requires an accurate determination of the modal characteristics of the structure at elevated temperatures. Modal surveys and ground vibration tests are routinely conducted at room temperature for supporting flutter analysis for subsonic and supersonic vehicles. Thermoelastic vibration tests for hypersonic vehicle applications, however, are not routinely performed for supporting flutter analyses, and are not well established, especially when compared to room-temperature techniques. Some prior research efforts in the area of thermoelastic vibration testing, predominantly with metallic materials, have been conducted for hypersonic vehicle applications over the past 40 years. These efforts investigated the effects of fundamental modal characteristics due to nonuniform heating on simple panels [2], simple wing structures [3-6] and a prototype wing for the X-15 vehicle [7]. Results indicated that the thermal stresses generated from heating a structure have significant degrading effects on structural stiffness (metallic materials) in addition to causing changes in material properties. Research from the X-30 National Aero-Space Plane [NASP] demonstrator model [8, 9] shows a destabilizing effect on flutter margins due to

material property degradation from heating over the hypersonic regime.

In recent years, numerous new high-temperature materials, new fabrication technologies and high-temperature sensors have been explored for hypersonic vehicle applications. These technology improvements increase the opportunities and need to develop advanced techniques for performing thermoelastic vibration testing. The new high-temperature materials increase in stiffness when heated. When these new materials are incorporated into a hot-structure, which also includes metallic components that decrease in stiffness when heated, the interaction between the two materials systems can affect the hypersonic flutter analysis. Performing a high-temperature modal survey will expand the research database for hypersonics and characterize this dual-material interaction.

The modal characteristics at room temperature need to be well-defined before attempting to understand the results and modal characteristics of the C/SiC RSTA high-temperature modal survey. Two series of room-temperature modal survey configurations were performed in the Flight Loads Laboratory [FLL] at NASA DFRC. The first configuration suspended the RSTA from a bungee cord for a free-free boundary condition; the second configuration mounted the RSTA to a strongback for a fixed boundary condition. Upon completion of the room-temperature modal surveys, modal response data was acquired while the RSTA was subjected to a simulated re-entry aerothermal heating environment.

2 Testing Facility

All three of the RSTA modal surveys were conducted at the NASA DFRC FLL, which offers thermal, structural, ground vibration and structural mode interaction testing of aircraft and aircraft components [10]. The FLL Large Nitrogen Test Chamber [LNTC] (shown in figure 3) provides a unique inert-atmosphere thermal testing capability.

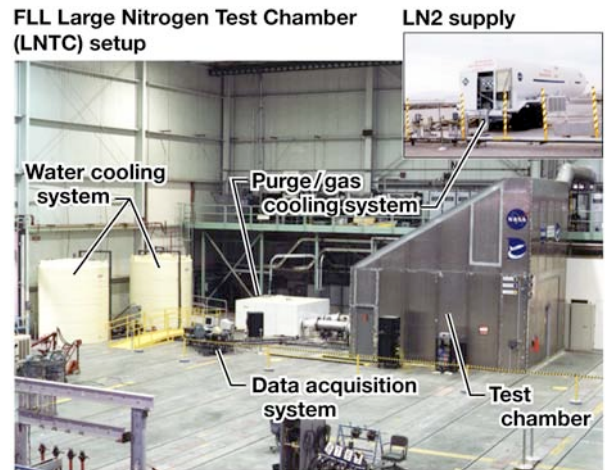


Fig. 3. The NASA Dryden Flight Research Center Flight Loads Laboratory Large Nitrogen Test Chamber.

The LNTC is a 20- by 24- by 20-ft (6.1- by 7.3- by 6.1-m) chamber capable of heating test articles to approximately 2500°F (1371°C) using quartz-lamp radiant heaters with active thermal control in an inert environment using nitrogen gas. The FLL maintains its own data acquisition and control system known as the Data Acquisition System (DACSIV) which monitors and records hundreds of sensors for the test facility operations. For dynamic and modal applications, the FLL utilizes a VTI Instruments Corporation (Irvine, California, USA) data acquisition system with capabilities up to 20,000 Hz at 51,200 samples per second.

3 Tests Description, Configuration and Objectives

Three RSTA modal survey configurations were performed at the NASA DFRC FLL in order to understand the hot-structure dual-material interaction that affects the structural integrity and modal characteristics of the test article during the re-entry aerothermal heating environment. The following outline presents the three RSTA modal survey test configurations that will be discussed in detail.

3.1) Room-Temperature Free-Free Test

- a. Sensor configuration: Room and high-temperature accelerometers
 - i. Impact hammer excitation
 - ii. Shaker excitation (Test 31)

- b. Sensor configuration: Only the high-temperature accelerometers
 - i. Impact hammer excitation
 - ii. Shaker excitation (Test 44)
- 3.2) Chamber Room-Temperature Strongback Test
 - a. Sensor configuration: Room and high-temperature accelerometers
 - i. Cable system installed (Test 6)
 - ii. Cable system removed (Test 15)
 - iii. Cable system reinstalled
 - b. Sensor configuration: Only the high-temperature accelerometers
 - i. Cable system installed
 - ii. Cable system removed (Test 38)
 - iii. Cable system reinstalled
- 3.3) Chamber Elevated-Temperature Strongback Test
 - a. Sensor configuration: Only the high-temperature accelerometers
 - i. Room-temperature test with no thermal systems running (Test 97)
 - ii. Room-temperature test with blowers and thermal systems running (Test 98)
 - iii. Elevated-temperature test
 - 1. Data acquired during thermal hold (Test 99)
 - 2. Data acquired during entire thermal profile (Test 109)
 - iv. Post-test room-temperature test with no thermal systems running

3.1 Room-Temperature Free-Free Modal Survey

The first RSTA modal survey was conducted in a free-free configuration at room temperature, with two objectives: to measure the structural frequencies in order to validate and provide the data needed to correlate the RSTA analytical finite element [FE] model, and to verify that the high-temperature accelerometers produced output similar to collocated room-temperature accelerometers. To simulate the free-free boundary condition needed to compare the test results with the FE model free-free results a “soft” boundary condition was created by hanging the RSTA from a bungee cord, as shown in figure 4.

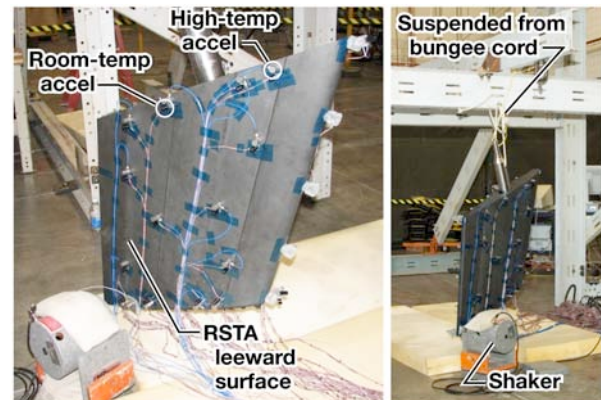


Fig. 4. The Room-Temperature Free-Free Test Setup.

The modal data were collected using 84 temporary external accelerometers on the RSTA surfaces. Two accelerometer types were used: room-temperature (maximum 150°F) (65.5°C) PCB Piezotronics (Depew, New York, USA) T333B ICP® (“Integrated Circuit - Piezoelectric”) accelerometers; and high-temperature (maximum 900°F) (482°C) PCB Piezotronics 357B61 charge accelerometers. The test article was excited on the leeward side and trailing edge in various locations and directions using two methods: an impact hammer and a 50-lb (22.6-kg) electromagnetic shaker using three force levels with burst random and sine sweeps (see figures 5 and 6). Both methods recorded the excitation input with a PCB Piezotronics 208A03 force transducer.

The RSTA had a total of 56 room-temperature accelerometers on the windward side, as shown in figure 5. There were 15 accelerometers on the spar box panels, 38 accelerometers on the structural spar boxes, and a tri-axial accelerometer on the spindle. All of the room-temperature accelerometers were mounted with hot glue in the appropriate orientation.

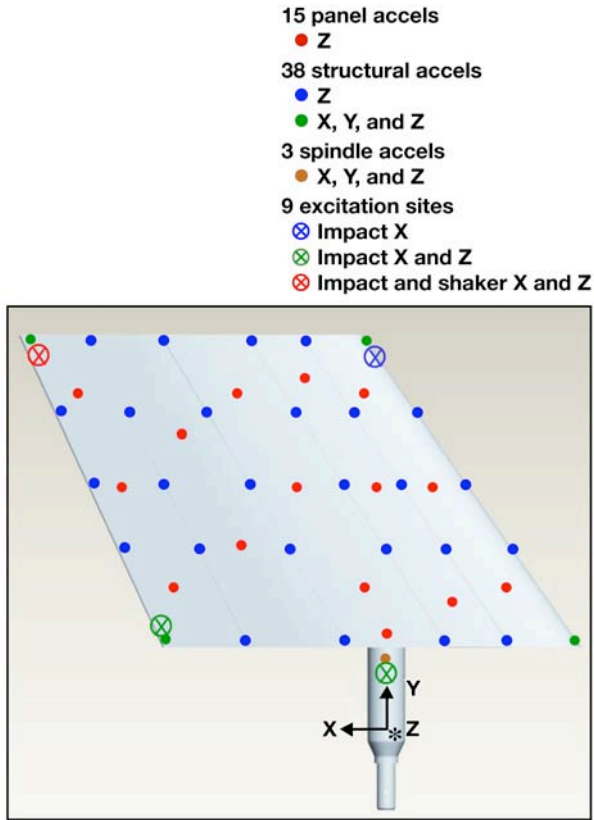


Fig. 5. The Accelerometer and Excitation Locations on the Windward Side for the Room-Temperature Free-Free Modal Survey.

The RSTA leeward side had a total of 28 accelerometers, as shown in figure 6. There were 14 high-temperature accelerometers located in existing RSTA screw holes along the structural spar boxes, and 14 collocated room-temperature accelerometers. Two factors limited the number of locations available for the high-temperature accelerometers. The first limiting factor was the requirement for a stud-mounted accelerometer installation to enable the follow-on thermoelastic vibration testing. The second limiting factor was that the existing RSTA screw holes necessary for mounting were only located along the sides of the spar boxes. The attachment method for the high-temperature accelerometers used specially-designed high-temperature stud mounts, torqued to RSTA installation requirements. Additionally, the collocated room-temperature accelerometers were mounted with hot glue.

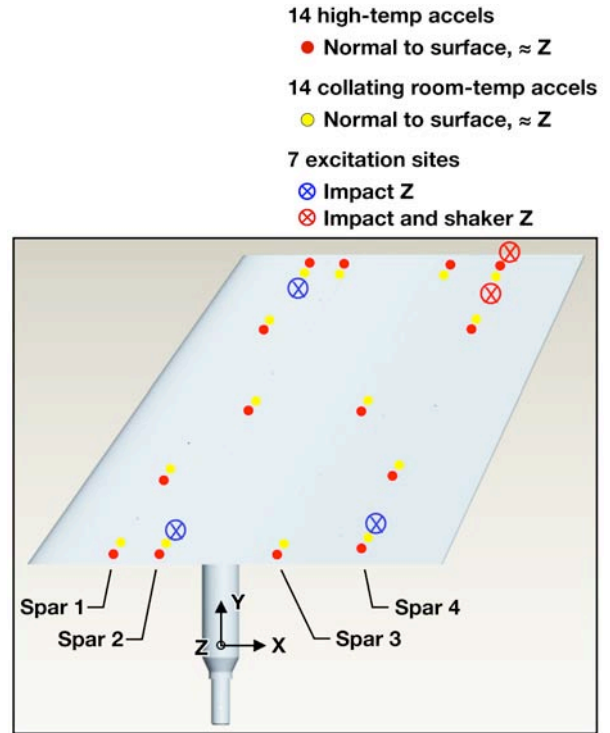


Fig. 6. The Accelerometer and Excitation Locations on the Leeward Side for the Room-Temperature Free-Free Modal Survey.

For the room-temperature free-free modal survey a total of 48 data runs were recorded between the two different excitation methods. A majority of the data sets used all 84 (room-temperature and high-temperature) accelerometers to capture the structural frequencies and mode shapes. Toward the end of the testing matrix all room-temperature accelerometers except the one on the tri-axial spindle were removed and data were collected with only the high-temperature accelerometers. These final tests with the high-temperature accelerometers characterized two effects: the frequency shift due to the mass effect of the room-temperature accelerometers, and the loss of fidelity of the mode shapes due to the limited RSTA screw hole locations for the high-temperature accelerometers.

3.2 Chamber Room-Temperature Strongback Modal Survey

The goal of the second modal survey was to obtain the RSTA structural frequencies and mode shapes at room temperature in the NASA DFRC FLL LNTC with the strongback fixed

boundary conditions. These modal data provided a baseline for the follow-on RSTA elevated-temperature modal tests with similar strongback boundary conditions. For this room-temperature modal survey the RSTA spindle was mounted onto the strongback in the bearing housing fixture in the LNTC without the heating oven and other heating hardware installed (see figure 7).

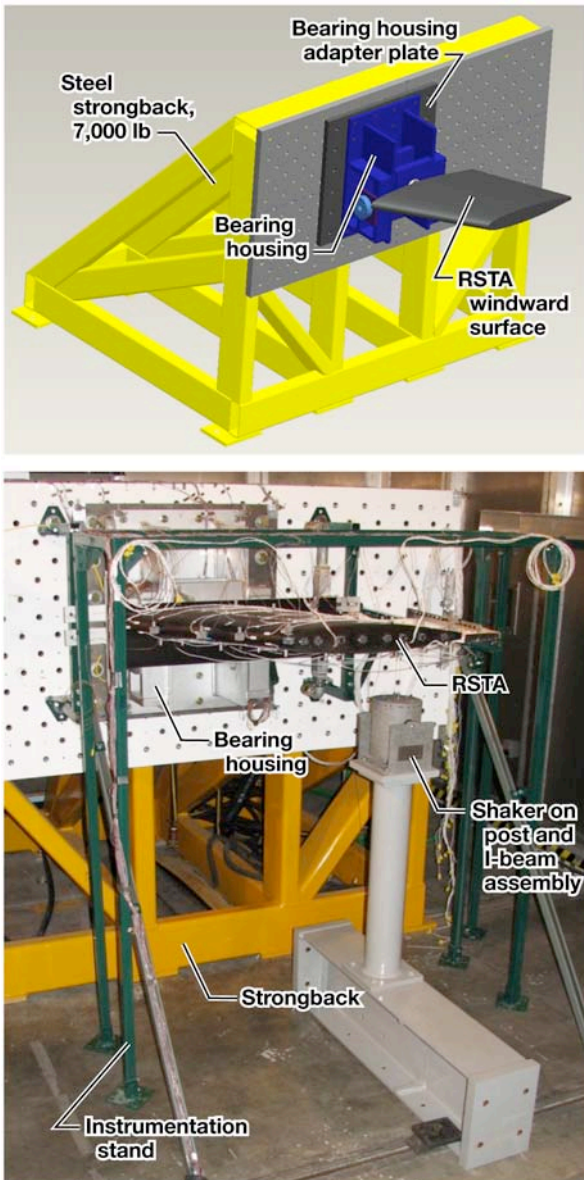


Fig. 7. The Chamber Room-Temperature Strongback Test Setup.

When mounting the RSTA onto the strongback extra effort was expended to try to make the boundary condition consistent from the room-temperature test to the subsequent

elevated-temperature modal survey. A 7,000-lb (3175-kg) steel strongback was secured to the floor tracks to accommodate the RSTA test setup. The RSTA Inconel® (Special Metals Corporation, Huntington, West Virginia, USA) spindle was cantilevered from two spherical bearings in the bearing housing; the bearing housing and bearing housing adapter plate were then bolted onto the strongback. Both rod ends in the crank link assembly had a spherical bearing to which the bearing housing provided a mounting surface for the load cell (see figure 8).

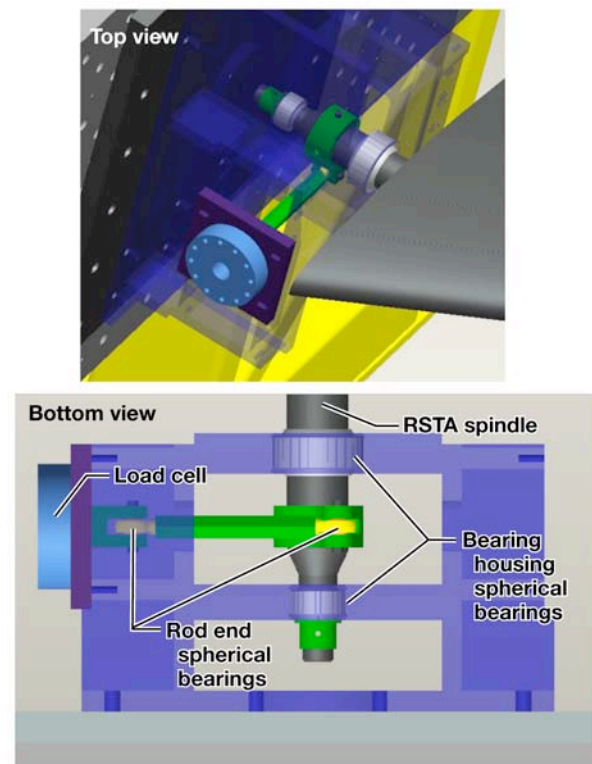


Fig. 8. The Spherical Bearings Inside the Bearing Housing and Rod Ends.

Once the RSTA was installed, a considerable amount of free play was found in the crank link assembly, allowing the RSTA outboard tip to rotate significantly beyond requirements. Hardware modifications were made to minimize the free play and although considerable improvements resulted, the problem was not eliminated. A cable system, shown in figure 9, was temporarily installed to eliminate the free play for the modal testing. Additional room-temperature modal test configurations were performed to evaluate

whether the cable system solution was repeatable and whether it was required for the room-temperature and elevated-temperature tests.

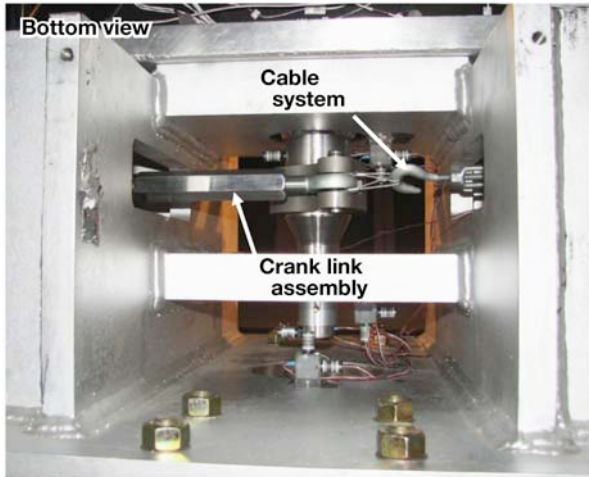


Fig. 9. The Temporary Cable System Installed to Eliminate Free Play.

Numerous factors required consideration during the design of the excitation setup to account for the thermal effects during the follow-on elevated-temperature modal testing, such as: the method of excitation within a thermal environment, the temperature limits on the electromagnetic shaker (maximum $\approx 100^\circ\text{F}$) ($\approx 37.7^\circ\text{C}$) and on the force transducer (maximum 400°F) (204°C), the limited access to the RSTA leeward surface because of the cold plate and other heating equipment, and other logistical challenges. The researchers decided to excite the RSTA using a 50-lb (22.6-kg) electromagnetic shaker with a modified excitation setup. This setup included a shaker securely mounted on a post-and-I-beam assembly providing burst random excitation in the vertical direction on the outboard aft spar box near the trailing edge of the leeward side of the RSTA. The modified shaker configuration is shown in figure 10.

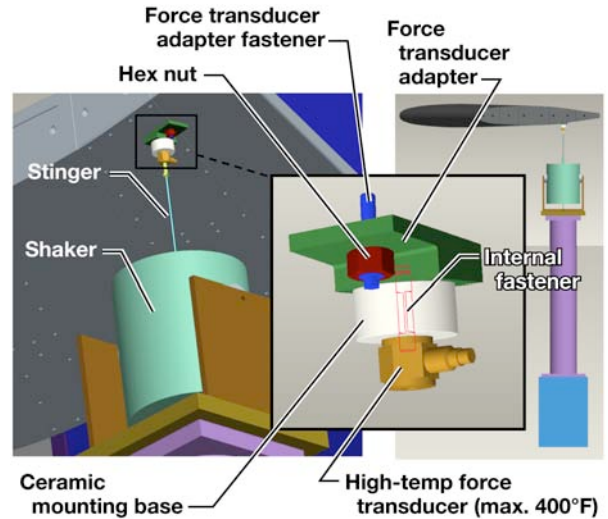


Fig. 10. The Modified Shaker Configuration.

The force transducer, which was a PCB Piezotronics 218C high-temperature (maximum 400°F) (204°C) charge sensor, could not be connected to the structure in the typical way for the elevated-temperature modal testing because of the RSTA leeward surface temperature exceeding the force transducer temperature limit, a clearance problem with the cold plate, and the available existing screw locations on the RSTA surface. A unique force transducer setup was designed to insulate and offset the transducer (see figure 10). A small hole was made in the water-cooled cold plate to allow the shaker stinger to pass through for the elevated-temperature testing while protecting the electromagnetic shaker from overheating. The shaker stinger was made from a high-temperature metal. The stinger alignment through the cold plate was critical for the elevated-temperature testing, but for the room-temperature modal survey the leeward cold plate was not installed. The force transducer adapter was designed at a slight angle to provide a vertical excitation, to provide the offset needed for the cold plate clearance and to connect to the leeward surface through an existing RSTA fastener location. A ceramic mounting base was placed between the force transducer adapter and the force transducer in order to insulate the sensor. A thermocouple was installed on the outer housing of the force transducer to monitor the thermal state.

The windward and leeward surfaces of the RSTA were instrumented with 47 room-temperature accelerometers and 14 high-temperature accelerometers, as shown in figure 11 and figure 12, respectively. These were used to fully characterize the entire test article since the high-temperature accelerometer installation was limited to the spar box. Thermocouples were installed on four of the high-temperature accelerometers to monitor temperatures during the thermal profiles for the follow-on elevated-temperature modal survey. The strongback and bearing housing were also instrumented with numerous room-temperature accelerometers in order to characterize the stiffness of the boundary condition and decouple the strongback modes from the RSTA modes.

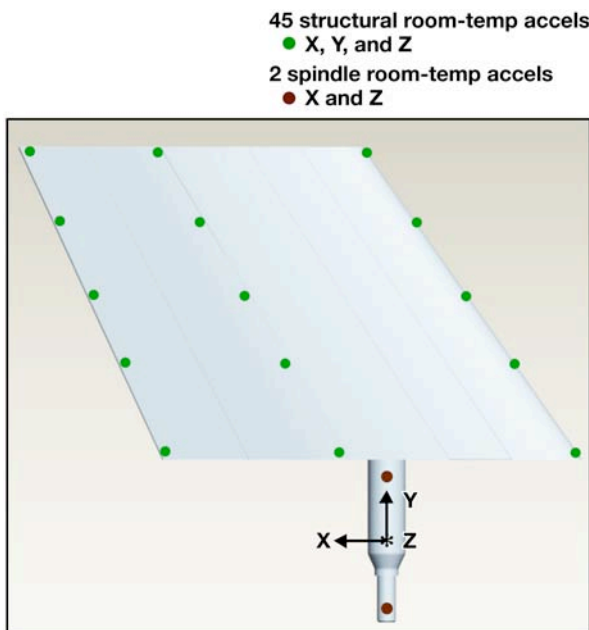


Fig. 11. The Accelerometer Locations on the Windward Side for the Chamber Room-Temperature Strongback Modal Survey.

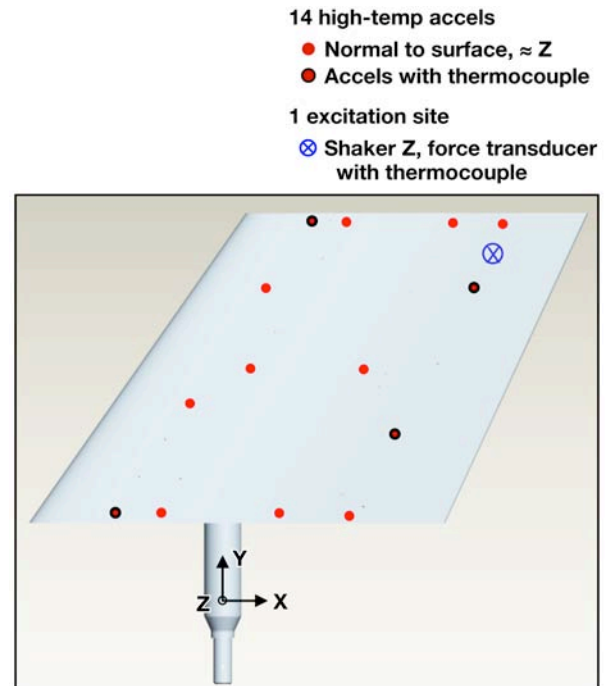


Fig. 12. The Accelerometer and Excitation Locations on the Leeward Side for the Chamber Room-Temperature Strongback Modal Survey.

For the chamber room-temperature strongback modal survey a total of 41 data runs were captured between the different free play and accelerometer configurations. For the first several configurations, all of the room-temperature and high-temperature accelerometers were installed to measure well-defined mode shapes. The cable system was initially installed, removed and then reinstalled to evaluate the free play problem that existed with the crank link assembly. The last configurations were tested with all of the windward surface room-temperature accelerometers removed except for the spindle accelerometers. A reassessment of the free play problem with the cable system installed and removed was also performed. These final test configurations with only the high-temperature accelerometers installed provided baseline mode shapes for the RSTA elevated-temperature modal tests.

3.3 Chamber Elevated-Temperature Strongback Modal Survey

The objective of the third modal survey was to acquire the structural frequencies and mode

shapes of the RSTA under a transient and spatially nonuniform thermal environment in the NASA DFRC FLL LNTC with the strongback fixed boundary conditions. The chamber elevated-temperature strongback test setup (see figure 13) was very similar to the chamber room-temperature strongback test setup except that all of the peripheral heating hardware was installed and the testing was conducted in an inert environment. The thermal profile for the RSTA thermoelastic vibration testing was developed to simulate the X-37 re-entry heating profile without exceeding the maximum temperature limit of the high-temperature accelerometers (maximum 900°F) (482°C). These modal data were the basis for understanding the material interaction between the C/SiC high-temperature material and the metallic spindle, as well as for obtaining some interesting findings concerning the high-temperature sensors.

survey was maintained as much as possible for the chamber elevated-temperature strongback testing so that direct comparisons could be made. The cold plate on the leeward side was installed for the chamber elevated-temperature test and provided insulation for the shaker. An alumina fiber thermal blanket was installed around the shaker for extra insulation. The oven heater stand, which housed the 36 windward and leading-edge high-density quartz-lamp radiant heaters and necessary hardware, was arranged in 22 thermal control zones. Using low excitation force levels for the room-temperature testing proved that the crank link assembly could be removed for the thermoelastic vibration testing since the free play did not influence the modal data. The locations of the leeward high-temperature accelerometers, force transducer, and the boundary condition room-temperature accelerometer were identical to those used in the previous room-temperature test. The high-temperature sensors that were predicted to experience the peak temperatures during the thermal profile, or possibly experience direct radiation, were insulated with a small amount of alumina blanket fibers. Thermocouples were installed on the outer canister of several of the insulated sensors to observe the temperature and ensure that the thermal profile developed for the modal survey did not exceed the maximum temperature limit of the sensors. To obtain and maintain an inert purged environment in the LNTC a very loud nitrogen blower system was used. The acoustical noise fluctuated as the nitrogen pressure in the chamber changed. The shaker excitation force level had to be slightly increased to bring the accelerometer modal data out of the acoustical noise. A noise dosimeter device was used to measure the acoustical levels inside the chamber during testing, and peaked at 145 dB when the chamber was fully pressurized.

For the elevated-temperature modal survey, numerous data runs were captured to characterize the test setup and acquire the desired thermoelastic modal data. Four parts were conducted for every attempt to gather elevated-temperature modal results. Part one consisted of conducting a room-temperature

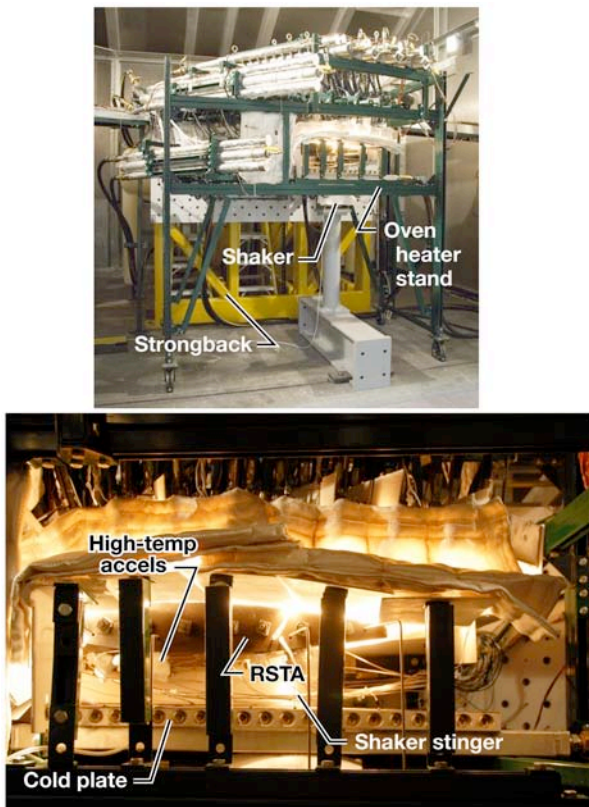


Fig. 13. The Chamber Elevated-Temperature Strongback Test Setup.

As previously stated, the setup used for the chamber room-temperature strongback modal

modal test the morning of the planned thermal modal run with no thermal systems operational. Part two involved conducting a room-temperature modal test once the chamber was fully purged and all of the thermal systems were functional, just prior to initiating the thermal profile. Part three acquired the desired thermoelastic modal data once the RSTA modal thermal profile was initiated. Part four involved taking a post-test room-temperature modal test with no thermal systems running once the RSTA cooled down. These four parts obtained the data necessary to track repeatability, characterize modal affects from the acoustics of the blower and thermal systems, directly evaluate thermal modal changes and evaluate the RSTA structure for permanent structural deformations resulting from the thermal loading.

Over the course of the elevated-temperature modal testing, two different time history data captures were acquired using the same thermal profile, as can be seen in figure 14. Initially, thermoelastic modal data were gathered at the peak profile temperature during a lamp heater temperature hold.

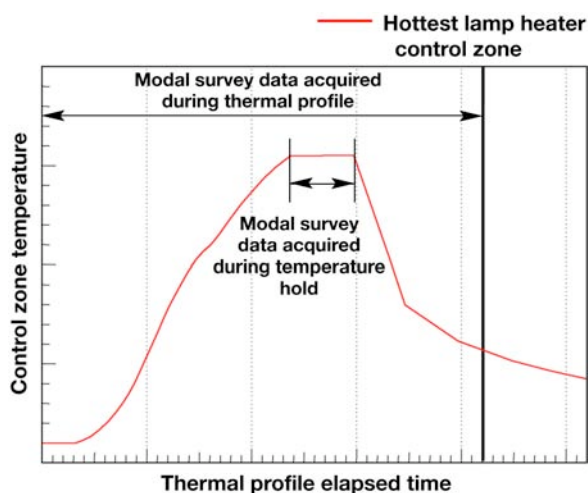


Fig. 14. The Thermal Profile for the Elevated-Temperature Modal Testing.

The RSTA continued to conduct heat throughout the structure during the hold for modal data collection and shortly into the cool-down process. This increased the surface temperatures significantly; however, the thermal profile designed for this modal test accounted for these effects to ensure that the

high-temperature sensors would not exceed the temperature limits. Multiple attempts to acquire modal data at this high-temperature hold were made, but only two successful thermal profiles were completed because of numerous failures with different systems of the LNTC. During the first successful thermal test, some questionable and undesirable effects were noticed regarding the high-temperature accelerometers despite them being within operating temperatures. These findings are discussed in the “Test Results” section below. Additionally, a time history data run throughout the entire thermal profile with continuous burst random excitation was successfully acquired. The elevated-temperature modal data provided some initial understanding of the material interaction between the C/SiC high-temperature material and the metallic spindle, but not all of the test objectives were met because of malfunctioning high-temperature modal sensors.

4 Test Results

The following sections describe the test results of the three RSTA modal surveys.

4.1 Room-Temperature Free-Free Modal Survey Results

For the room-temperature free-free modal survey a total of 48 data runs were recorded using the impact hammer and shaker excitation methods at various locations and in various directions. Exciting the test article with the 50-lb (22.6-kg) electromagnetic shaker provided improved results over exciting the test article with the impact hammer. Each shaker excitation location used three force levels; however, the smallest input force resulted in the cleanest data.

A comparison was made between two data runs of similar input forces using burst random excitation with different accelerometer configurations. Test 31 utilized all 84 room-temperature and high-temperature accelerometers installed on the RSTA to capture the structural frequencies and detailed mode shapes. Test 44 utilized only the tri-axial room-temperature spindle accelerometer and

14 high-temperature accelerometers to capture a limited set of structural frequencies and mode shapes, because of the limited RSTA spar screw hole locations available for the high-temperature accelerometers. The mass difference from removing all of the room-temperature accelerometers and associated cables prior to test 44 was approximately 2.5 lb (1.1 kg), which significantly influenced the frequencies of the 68-lb (30.8-kg) test article. Figure 15 shows a frequency response function [FRF] that illustrates the frequency shift during test 31 and test 44 of the accelerometers in the same general location along the root of the third spar. These RSTA third-spar root sensors included windward room-temperature, leeward high-temperature and collocated leeward room-temperature accelerometers. The frequency trend is very similar between the two tests; the increased frequencies shown on the high-temperature accelerometer for test 44 were expected after the removal of all of the room-temperature accelerometers. One can also see from this FRF that the leeward high-temperature and collocated room-temperature accelerometers show nearly exact frequency content at all peaks for test 31. This is an exceptional result since these high-temperature PCB Piezotronics 357B61 charge accelerometers had never been used before by DFRC personnel or directly compared with the DFRC standard ground-testing room-temperature PCB Piezotronics T333B ICP accelerometers. The sensitivity and other specifications of the two different types of accelerometers were significantly different; however, the only noteworthy difference is that the charge accelerometer data are noisier overall, especially at the antinodes.

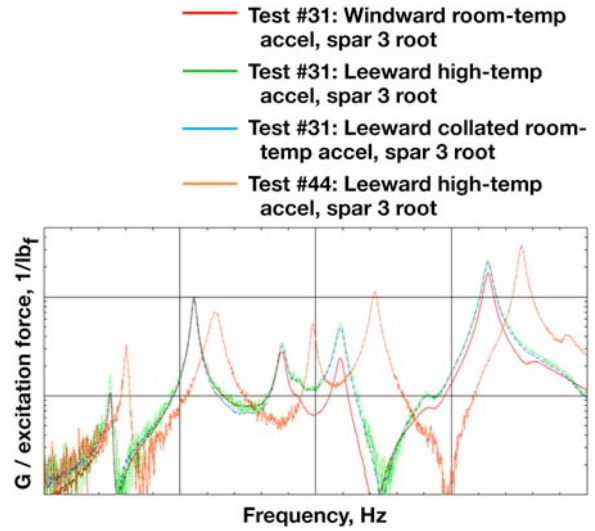


Fig. 15. The Frequency Response Function, Illustrating Frequency Shifts.

The FRF shown in figure 16 illustrates the importance of the placement of the accelerometer location and direction to truly capturing all structural frequencies and mode shapes. Many of the windward room-temperature accelerometers were installed in all three X, Y, and Z directions; however, the installation of the high-temperature accelerometers was limited normal to the leeward surface, or very close to the Z direction, in available RSTA screw hole locations. Several of the RSTA mode shapes were deformed only in the X and Y directions; the leeward high-temperature and collocated room-temperature accelerometers were limited to capturing only the structural frequencies and mode shapes in the Z direction, therefore not portraying the entire modal characteristic of the test article.

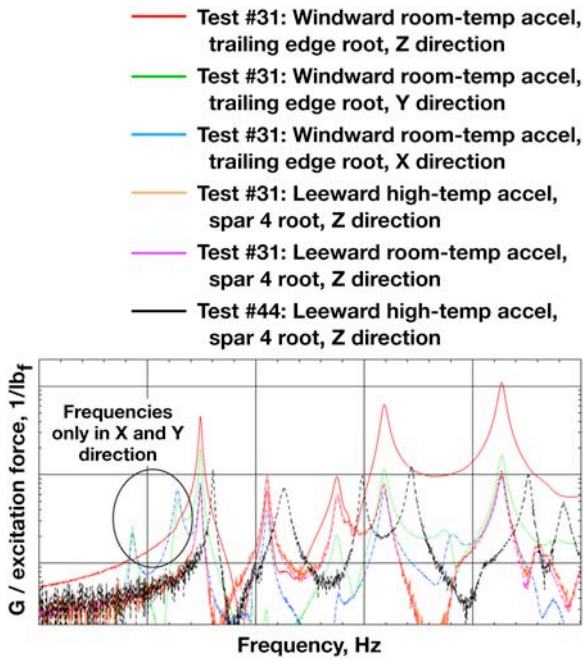


Fig. 16. The Frequency Response Function, Illustrating the Importance of Sensor Placement.

The results shown in figure 17 compare the frequency difference between modes measured during test 31 and test 44. The frequency difference shown is caused by the combination of the limited placement and direction of the high-temperature accelerometers and the mass effect of the removed accelerometers.

Test #31 mode shape	Test #44 mode shape	Percent freq. difference
1	Not found	–
2	Not found	–
3	Not found	–
4	Not found	–
5	Not found	–
Not found	1	–
6	2	4.5
7	3	1.2
8	4	5.0
9	Not found	–
10	Not found	–
11	5	3.1
12	6	5.7
13	Not found	–
14	7	4.5
15	8	4.5
16	9	4.4

Fig. 17. The Percent Frequency Differences from Test 31 and Test 44.

Figure 18 compares the mode shapes between test 31 and test 44 overlaid on the test model with the spindle. The left side of figure 18 shows the reduced-order mode shape from a polyreference curve fit from test 44 using the high-temperature accelerometers. The right side of figure 18 shows two mode shapes using a polyreference curve fit of all of the accelerometers from test 31. The top right shows the detailed, fully-characterized mode shape from all room-temperature and high-temperature accelerometers on the test model. The bottom right shows the mode shape on the reduced-order test model with only the spindle and high-temperature accelerometers, a direct comparison to the mode shape of test 44 (on the left side).

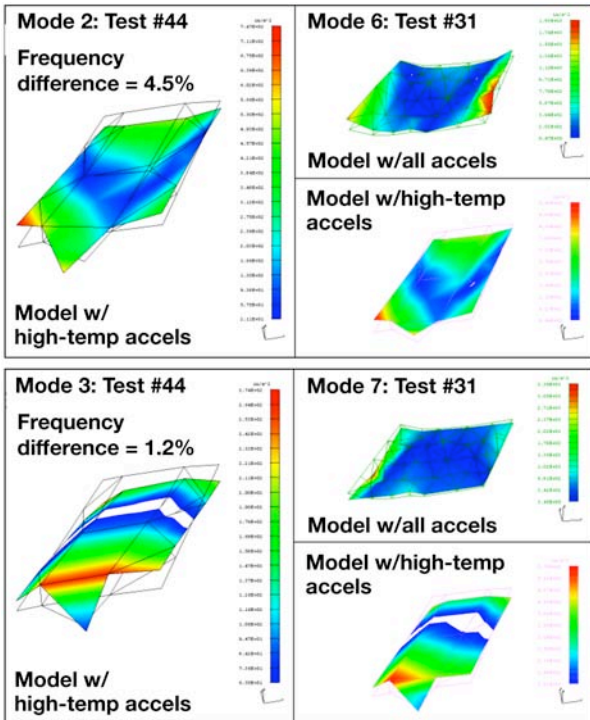


Fig. 18. Mode Shape Comparison from Test 31 and Test 44.

All of the objectives of the room-temperature free-free modal survey were achieved with the successful measurement of the frequencies and mode shapes necessary to validate and correlate the RSTA analytical FE model, as well as verifying that the high-temperature accelerometers produced similar output to the collocated room-temperature accelerometers.

4.2 Chamber Room-Temperature Strongback Modal Survey Results

For the chamber room-temperature strongback modal survey a total of 41 data runs were captured between the different free play and accelerometer configurations. These data runs used an electromagnetic shaker that was vertically mounted with four force levels in the same excitation location on the outboard, aft spar box near the trailing edge of the leeward side of the RSTA.

Multiple data runs were evaluated and compared to assess the free play problem found in the crank link assembly and how it directly affected the RSTA frequencies. Figure 19 shows an FRF comparison of the same high-

temperature accelerometer for test 6, during which the free play in the crank link assembly was eliminated by installing the temporary cable system, and test 15, during which the cable system was removed and the free play was present. At the lower, more desirable, frequency range, the frequency data are not affected by the increased stiffness of the cable system which eliminated the free play; however, in the higher, less-important frequency range of the RSTA the frequency values were slightly changed. The required load to overcome the free play was much higher than the ideal shaker excitation input force, and the researchers decided that the cable system would not be used for the elevated-temperature testing.

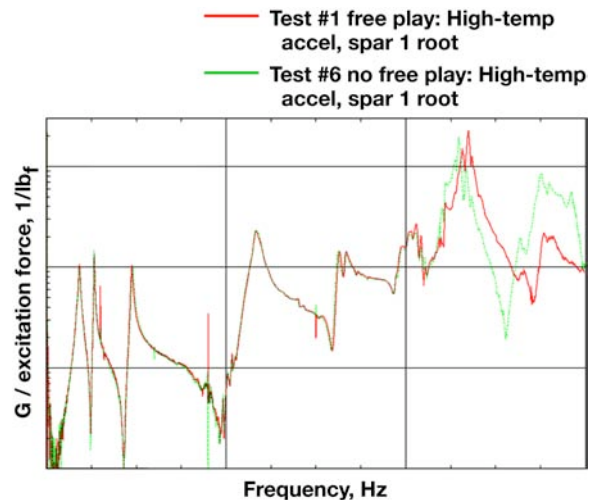


Fig. 19. The Frequency Response Function, Free Play Comparison from Test 6 and Test 15.

Test 15 and test 38 used a burst random excitation with similar input forces; the cable system was not used. The difference between the two tests was the accelerometer configuration. Test 15 used all of the 47 windward room-temperature accelerometers and 14 leeward high-temperature accelerometers installed on the RSTA surfaces in order to fully characterize the modal response of the entire test article. Test 38 used only the tri-axial room-temperature spindle accelerometer and the 14 high-temperature accelerometers on the leeward surface. This captured the limited structural frequencies and mode shapes due to the restricted RSTA screw

hole locations for the high-temperature accelerometers. The modal data from test 38, with only the high-temperature accelerometers, provided baseline mode shapes for the RSTA elevated-temperature modal tests. As expected, the mass difference from removing all of the windward room-temperature accelerometers for test 38 significantly influenced frequencies. Figure 20 shows an FRF comparing the frequency shift from test 15 and test 38 using the same high-temperature accelerometer on the first spar tip of the RSTA. The frequency trend is very comparable between the two tests and the increased frequencies shown for test 38 were a result of the mass reduction of removing the room-temperature accelerometers.

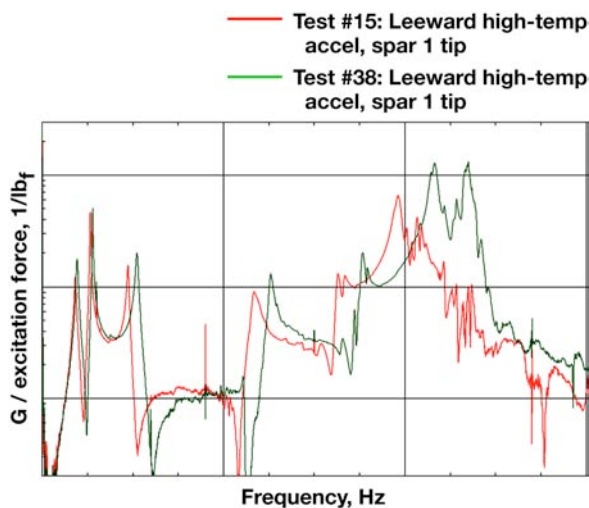


Fig. 20. The Frequency Response Function, Frequency Shift due to Sensor Mass, from Test 15 and Test 38.

Consistent with the room-temperature free-free modal survey, the accurate placement of an accelerometer location and direction is needed to truly capture all modal characteristics. The leeward high-temperature accelerometers along the edge of the spar boxes were limited to capturing only the structural frequencies and mode shapes in the vertical direction of the test article in the fixed boundary condition of the strongback. Figure 21 shows an FRF comparing a tri-axial room-temperature accelerometer on the tip trailing edge of the RSTA for test 15 to a high-temperature accelerometer in only the Z direction on the fourth spar tip of the RSTA for test 38. As expected, test 38 is missing the

frequencies from mode shapes dominated by X and Y displacements due to the limited placement and direction of the high-temperature accelerometers.

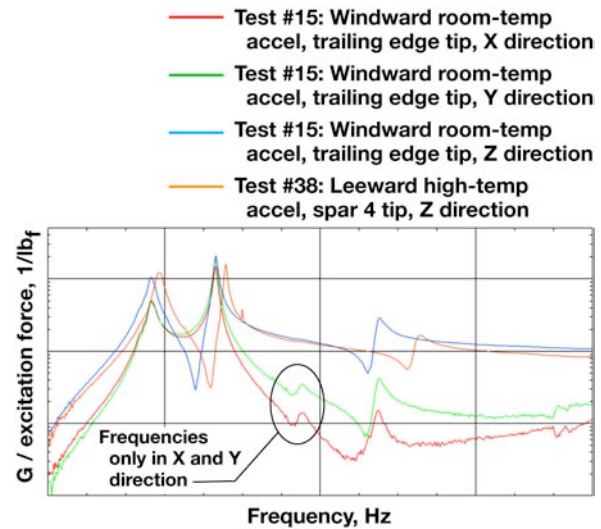


Fig. 21. The Frequency Response Function, Missing Frequencies due to Sensor Placement, from Test 15 and Test 38.

The results shown in figure 22 compare the frequency difference between modes measured during test 15 and test 38. The frequency difference shown is due to the combination of the limited placement (direction) of the high-temperature accelerometers and the mass effect of the removed accelerometers. The mode shapes on white background from test 38 are the correlated, well-defined mode shapes that represent the baseline data for comparison to the RSTA elevated-temperature modal tests.

Test #38 mode shape	Test #15 mode shape	Percent freq. difference	How test #38 mode shapes match to test #15
1	1	5.1	Excellent
2	2	4.5	Excellent
3	3	9.5	Excellent
4	6	-16.9	Good
5	Not found	-	N.A.
6	Not found	-	N.A.
7	9	8.1	Excellent
8	10	4.4	Fair
9	11	1.2	Poor
10	12	0.3	Excellent
11	13	0.2	Good
12	15	7.5	Good
13	16	5.3	Good
14	17	5.7	Excellent
15	18	5.0	Excellent
16	19	7.4	Good
17	20	6.5	Excellent
18	21	2.8	Excellent
19	23	0.3	Good
20	25	-2.3	Fair
21	24	1.7	Excellent
22	22	6.4	Good
23	Not found	-	N.A.
24	27	8.8	Good
25	28	5.9	Excellent

Fig. 22. The Percent Frequency Differences from Test 15 and Test 38.

Figure 23 visually compares the mode shapes between test 15 and test 38 overlaid on the test model with the spindle. The left side of the figure shows the reduced-order mode shape from a polyreference curve fit of the modal data from test 38 using the high-temperature accelerometers. The right side of the figure shows two mode shapes using a polyreference curve fit of all of the accelerometers from test 15. The top right shows the detailed, fully characterized mode shape in the strongback boundary condition from all room-temperature and high-temperature accelerometers shown on the test model; the bottom right shows the

mode shape displayed on the reduced-order test model with only the spindle and high-temperature accelerometers, a direct comparison to the mode shape of test 38 (on the left side).

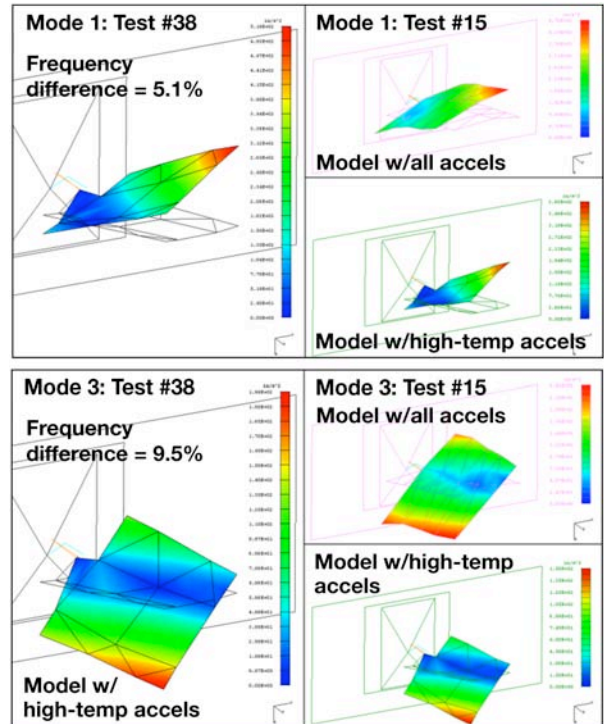


Fig. 23. Mode Shape Comparison from Test 15 and Test 38.

The objectives of the second RSTA modal survey were met by measuring the RSTA structural frequencies and mode shapes at room temperature in the NASA DFRC FLL LNTC with the strongback fixed boundary conditions. Test 38 provided baseline data for the follow-on RSTA elevated-temperature modal tests with similar strongback boundary conditions.

4.3 Chamber Elevated-Temperature Strongback Modal Survey Results

For the chamber elevated-temperature strongback modal survey a total of three successful thermal data runs were captured. Two of the modal data runs recorded were with burst random excitation during the high-temperature hold of the thermal profile and the third data run collected was with a continuous burst random excitation during the entire simulated RSTA re-entry thermal profile.

All data runs consisted of the same high-temperature accelerometer configuration and the same excitation location previously used for the chamber room-temperature strongback modal test. There were four parts to each successful elevated-temperature modal test.

Modal data were gathered with 30 frames of burst random excitation during the first successful thermal chamber operations. During the hold portion of the thermal profile some questionable and undesirable effects were seen in the output of the high-temperature accelerometers. A second thermoelastic modal test with data acquired during the thermal hold was conducted to verify repeatability of the questionable high-temperature accelerometer output. Finally, a third modal test with 360 frames of continuous burst random excitation through the entire thermal profile was performed to further study the questionable output of the high-temperature sensors. Thermocouples verified that the questionable sensors were within operating limits during all three thermoelastic tests.

The left side of figure 24 shows time history plots of the response from three different accelerometers from the first successful high-temperature data acquisition (test 99) during the entire thermal hold. The right side of figure 24 also shows time history plots, these of the response from three different accelerometers captured during the thermal profile of test 109. Both tests show that the high-temperature sensors are undergoing possible thermal effects as the accelerometers are getting hotter. The top plots from both tests show an accelerometer response in a cooler region on the leeward surface and little to no thermal effects in the output. The hotter mid-range sensors seen in the middle plots for both tests exhibit a questionable unsteady offset in the time history data. The continuous excitation data show a region during the thermal profile in which the sensor output was extremely dense for many data frames. The data were never lost, but do fail to follow the excitation bursts and are most likely erroneous. The lower plots show an accelerometer response on the RSTA leeward surface in the hottest region, in which the sensor experienced complete and

intermittent data dropouts for numerous data frames during the higher temperatures of the thermal profile. The continuous excitation data also show this effect, but the intermittent accelerometer returns to operational status once the sensor experiences a lower temperature range. The researchers speculate that the malfunction was most likely due to the intense ramp-up rate of the thermal re-entry profile. Sensor manufacturers do not product-test these high-temperature accelerometers with the extreme thermal ramp rates required to simulate hypersonic re-entry thermal profiles. All high-temperature accelerometers continued to function normally in later room-temperature tests, concluding that the sensors were malfunctioning in response to some type of thermal effects.

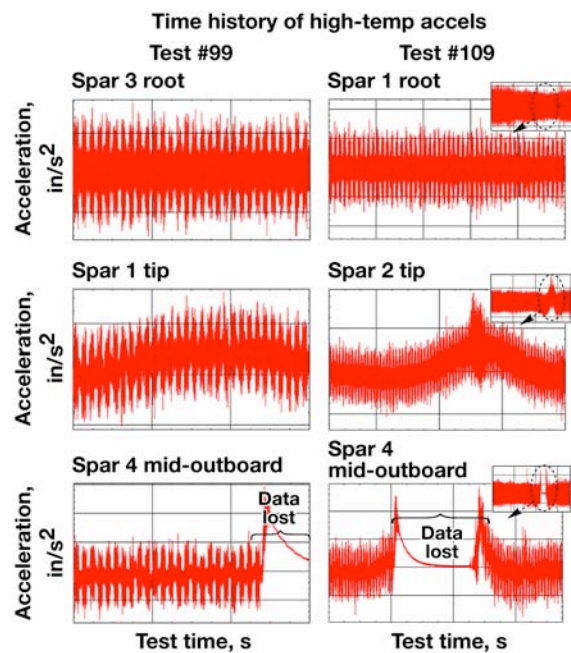


Fig. 24. Time History for High-Temperature Accelerometers from Test 99 and Test 109.

Figure 25 further illustrates this questionable thermally-induced behavior in the response of the hottest accelerometer located mid-outboard on the fourth spar of the RSTA for test 99 during the thermal hold portion of the thermoelastic modal test. Temperature output from during the thermal hold for the thermocouples installed on several of the high-temperature sensors is also shown with the shaker excitation and accelerometer response

superimposed. For this test, this particular accelerometer had dropout data for approximately 11 of the 30 frames acquired. An unusual characteristic of these data is that the sensor returned to operational status with the unsteady offset effect even though it continued to heat up.

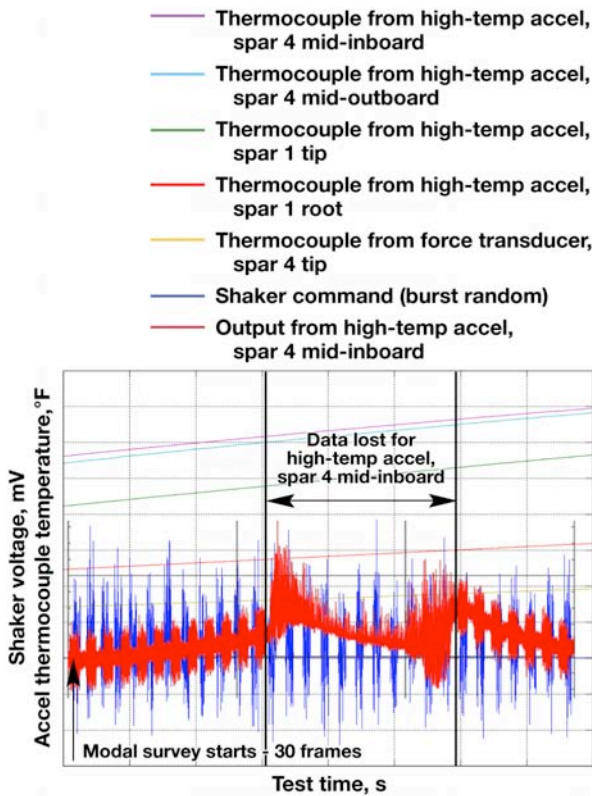


Fig. 25. Time History for Thermocouples, Shaker Command and One High-Temperature Accelerometer Output from Test 99.

Post-processing and analyzing the thermoelastic modal data with intermittent data dropouts occurring at different times on different accelerometers was extremely difficult. A high number of simultaneous data frames of all of the high-temperature sensors are needed to properly capture the modal data necessary for creating mode shapes. As is shown in figure 26, some direct FRF comparisons with the thermal effect can be made for the high-temperature accelerometers that were in the cooler regions of the RSTA during the thermal profile. This figure shows data from a high-temperature accelerometer located on the mid-inboard first spar of the RSTA leeward surface for room-temperature

test 97 and test 98, which were conducted prior to the elevated-temperature test, as well as for elevated-temperature modal survey test 99. It is apparent that during test 98 and test 99 (the room-temperature and elevated-temperature tests with the nitrogen chamber purged and blowers fully functional) the modal data are very noisy and exhibit a distinct frequency spike in response to the acoustical influence of the blower. The room-temperature data with the blower frequency do, however, adequately correlate with the room-temperature no-blower data. With the noise present on the accelerometer signal from the blower acoustics the sensor is still capable of accurately estimating the modal frequencies. A frequency difference can also be seen, mainly with the middle and higher modes, because of the thermal stresses created during the simulated RSTA re-entry thermal profile. It is difficult to directly correlate the thermoelastic frequency differences seen in the FRF to the room-temperature frequencies without being able to visualize the mode shapes to ensure correct frequency comparisons are being made; however, it is evident from the elevated-temperature modal data that the hot-structure control surface experiences some structural stiffness changes from the thermal loading, as expected from theory.

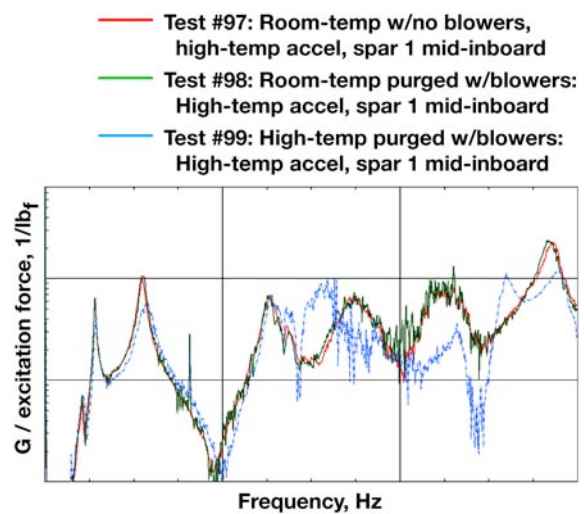


Fig. 26. The Frequency Response Function, Thermoelastic Frequency Shift from Tests 97, 98 and 99.

The modal test results from unsuccessful thermal operational attempts in which the

complete thermal profile was not implemented indicate that the thermal stresses significantly depend on the manner in which the test article was heated, as expected. The higher the heating rate, the more the thermal gradient will build up in the test article, which drives the thermal stresses. In order to properly capture the structural stiffness changes, extreme care needs to be taken to accurately simulate the aerodynamic heating of a hypersonic re-entry vehicle when performing laboratory radiant heating tests.

The objectives of the third RSTA modal survey to acquire the frequencies and mode shapes under a transient and spatially nonuniform thermal environment with the strongback fixed boundary conditions were not completely obtained because of a deficient set of functional high-temperature accelerometer responses. Therefore, the hot-structure control surface material interaction between the C/SiC high-temperature material and the metallic spindle could not be fully analyzed and understood. Even with incomplete data, this research on a hot-structure control surface verifies a similar trend to the prior metallic material research, wherein the thermal stresses generated from a thermal profile have a significant effect on the structural stiffness and modal properties.

5 Conclusion and Future Work

During the course of the effort to conduct an elevated-temperature modal survey, numerous lessons were learned that can improve the development of future techniques for carrying out hypersonic modal applications. The prevailing setback during the elevated-temperature modal testing was that the high-temperature accelerometers on the hotter region of the test article malfunctioned. Lacking a complete set of high-temperature accelerometer responses, not all of the final test objectives could be met to fully understand the material interaction between the carbon-silicon carbide high-temperature material and the metallic spindle. In response to the malfunctioning high-temperature accelerometers, however, several steps need to be taken to understand the

complexity of these sensors and improve their functionality during thermoelastic vibration tests. Additional evaluation and comparison tests of the high-temperature sensors used in the Ruddervator Test Subcomponent Article testing as well as other available high-temperature sensors need to be conducted to enable high-temperature modal survey tests.

Another major obstacle for hypersonic applications that requires research is the time-varying nature of the thermoelastic modal data. Structural frequencies vary during the course of the thermal profile; at the present time it is not certain what the best analytical methods are to update and validate FE models or perform hypersonic flutter analyses while accounting for these thermal and structural time-varying characteristics.

Acknowledgement

The author thanks Materials Research & Design, Inc. [MR&D] of Wayne, Pennsylvania, for conducting numerous thermal and modal analyses in preparation for the RSTA modal surveys, as well as the NASA DFRC Flight Loads Laboratory technicians and other NASA RTSA engineering personnel for their assistance in setting up and performing the operations for the modal surveys.

Copyright Statement

The authors confirm that they, and/or their company or organization, hold copyright on all of the original material included in this paper. The authors also confirm that they have obtained permission, from the copyright holder of any third party material included in this paper, to publish it as part of their paper. The authors confirm that they give permission, or have obtained permission from the copyright holder of this paper, for the publication and distribution of their paper as part of the ICAS2010 proceedings or as individual off-prints from the proceedings.

References

- [1] The Boeing Company. X-37B orbital test vehicle. http://www.boeing.com/defense-space/ic/sis/x37b_otv/x37b_otv.html, accessed May 20, 2010.

HIGH-TEMPERATURE MODAL SURVEY OF A HOT-STRUCTURE CONTROL SURFACE

- [2] Vosteen, Louis F and Fuller, Kenneth E. Behavior of a cantilever plate under rapid-heating conditions. NACA RM-L55E20c, 1955.
- [3] Vosteen L, McWithey R and Thomson R. Effect of transient heating on vibration frequencies of some simple wing structures. NACA Technical Note 4054, 1957.
- [4] Kehoe M and Snyder H. Thermoelastic vibration test techniques. NASA Technical Memorandum 101742, 1991.
- [5] Snyder H and Kehoe M. Determination of the effects of heating on modal characteristics of an aluminum plate with application to hypersonic vehicles. NASA Technical Memorandum 4274, 1991.
- [6] Kehoe M and Deaton V. Correlation of analytical and experimental hot structure vibration results. NASA Technical Memorandum 104269, 1993.
- [7] McWithey R and Vosteen L. Effects of transient heating on the vibration frequencies of a prototype of the X-15 wing. NASA Technical Note D-362, 1960.
- [8] Heeg J, Gilbert M and Pototzky A. Static & dynamic aeroelastic characterization of an aerodynamically heated generic hypersonic aircraft configuration. NASA N91-N10320, 1990.
- [9] Heeg J, Zeiler T, Potozky A, Spain C. and Englund W. Aerothermoelastic analysis of a NASP demonstrator model. NASA Technical Memorandum 109007, 1993.
- [10] National Aeronautics and Space Administration. Flight Loads Laboratory (FLL) <http://www.aeronautics.nasa.gov/atp/facilities/fl/index.html>, accessed May 20, 2010.